Biofilm Adhesion to Surfaces is Modulated by Biofilm Wettability and Stiffness

Martin Kretschmer, Carina Anke Schüßler, and Oliver Lieleg*

Although many surfaces in industry and medicine are colonized by bacterial biofilms, little is known about the physical principles that govern the adhesion properties of such bacterial communities. In part, this is due to the technical challenge associated with the characterization of a biofilm directly on the substrate it is grown on. Moreover, distinguishing between the cohesive and adhesive properties of a (bio)material requires information on the amount of material transferred between the interacting surfaces, which is not easily possible in existing measurement techniques applied in biofilm research. Here, a new method is introduced which allows for characterizing the detachment process of biofilms in situ and makes it possible to identify the dominant mode of fracture. As a countersurface in those detachment tests with biofilm layers, either a synthetic/inorganic material surface or another biofilm layer can be used. By comparing results obtained with different biofilms generated at distinct cultivation conditions, how two selected material properties, i.e., the biofilm wettability and the biofilm stiffness, contribute to the detachment process can be shown. The novel measurement approach demonstrated here can easily be adapted further to enable adhesion/detachment measurements with a broad range of other biofilms including those grown at submerged conditions.

1. Introduction

Bacteria form slimy substances, so-called biofilms; this allows them to settle permanently on surfaces[1–4] and to protect themselves from external challenges, such as temperature differences, toxic substances or shear loads.[5–9] Biofilms are able to adhere to nearly any surface in a wet environment; examples include pipes, ship hulls, teeth or medical implants.[10–15] Biofilms contain not only bacteria but also extracellular polymeric substances (EPS) secreted by them.[16–18] Typically, the EPS comprises polysaccharides, proteins and extracellular DNA.[19–22] Whereas many studies have investigated the adhesion of individual bacterial cells to surfaces,[23–27] less is known how the biofilm matrix contributes to this phenomenon.[28–31] There are, however, strong indications that the biofilm matrix polymers play an important role here as well:[32,33] cross-linking of the biofilm matrix by, e.g., metal ions, has been shown to strongly alter the viscoelastic properties, cohesion strength and erosion resistance of biofilms;[34–37] it appears likely that those material properties are closely related to the adhesion behavior of biofilms.

Different techniques have already been established to quantify certain material properties of biofilms. For instance, macrorheology is very well suited to investigate the shear stiffness and yielding behavior of viscoelastic materials such as biofilms[38–41]—and such measurements allow for drawing conclusions on the cohesion behavior of these slimy substances. Classical macrorheological measurement protocols, however, cannot assess the surface adhesion properties of biofilms, and standardized procedures to characterize this surface adhesion behavior of biofilms do not exist yet.

In contrast, for synthetic materials such as glues, there are well-defined protocols for quantifying their adhesion and cohesion strength:[42] Those either apply stretching forces in the vertical direction thus measuring the tensile strength of a material,[43] or they make use of large shear forces to study the internal yielding behavior of a glue.[44,45] Other methods apply torsional forces to a sample to generate a defined shear stress, e.g., by rotating the two opposing surfaces relative to each other.[46] With the latter protocols (which can, in similar form, easily be implemented in a standard rheometer), however, drawing conclusions on the adhesion properties of a material is not easily possible. In addition, standard procedures developed for testing synthetic glues would require a biofilm (prior to its characterization) to be removed from the substrate it was grown on—and this can significantly affect the result of an adhesion measurement.

There are, however, a few examples of dedicated setups which allow for investigating the adhesive properties of biofilms in situ. For instance, Chen et al. characterized the adhesion

M. Kretschmer, C. A. Schüßler, Prof. O. Lieleg
Department of Mechanical Engineering and Munich School
of Bioengineering
Technical University of Munich
Boltzmannstraße 11, 85748 Garching, Germany
E-mail: oliver.lieleg@tum.de
M. Kretschmer, C. A. Schüßler, Prof. O. Lieleg
Center for Protein Assemblies (CPA)
Technical University of Munich
Ernst-Otto-Fischer Straße 8, 85747 Garching, Germany

The ORCID identification number(s) for the author(s) of this article can be found under https://doi.org/10.1002/admi.202001658.

behavior of biofilms by removing them from their substrate with a spatula and measuring the lateral force occurring during this scraping process.[47] A different approach was chosen by Yan et al., who employed capillary forces to remove biofilms from a surface to measure the corresponding adhesion energy.[48] With this method, the biofilm layer remains intact can be transferred to a different substrate and—potentially—be characterized further. In spite of this considerable progress made in the area of biofilm adhesion, there is no clear picture yet if and how biofilm detachment from a surface is linked to other material properties of this bacterial substance.

Here, we present a measurement setup based on a commercial rheometer, which applies normal forces to the biofilm material and allows for characterizing the detachment process of biofilms from the substrate they are grown on. Since we can analyze both, the force–distance curves measured during the detachment process and the amount of biological material transferred between the two test surfaces, we can differentiate between an adhesive and cohesive failure of the biomaterial. Moreover, we are able to test this detachment process in two different configurations, i.e., in a metal-on-biofilm and a biofilm-on-biofilm setup. We compare biofilms generated by three different variants of the soil bacterium *Bacillus subtilis* and alter the biofilm properties by modulating the nutrient conditions during biofilm growth or exposing the biofilm to cross-linking metal ions. Our results demonstrate that the wetting properties of a biofilm and—to a lesser extent—the biofilm stiffness dictate the detailed detachment behavior of biofilms by deciding whether adhesion or cohesion failure dominates.

2. Experimental Section

2.1. Development of a New Measurement Method to Characterize the Adhesion and Cohesion of Mature Biofilms In Situ

The technique introduced here allows for quantifying the adhesive properties of a biofilm toward a second surface, which can either be a metal surface (here aluminum) or another biofilm layer. This is made possible by equipping a commercial rheometer (MCR 302; Anton Paar GmbH, Graz, Austria) with a custom-made measuring head (**Figure 1**a) and sample holder (Figure 1c). Technical drawings of the custom-made components for the detachment test are shown in the Supporting Information (Figures S1–S5, Supporting Information).

The dedicated measuring head is used when a biofilm-on-biofilm configuration is tested; otherwise, a commercial planar measuring head (made from aluminum) with a diameter of 25 mm is used (D-PP25/AL/S07, No. 10637, Anton Paar). The custom-made measuring head comprises three components made from polytetrafluoroethylene (PTFE): a ring, a cup and a connector pin. The ring can be attached to the cup with six screws and the pin is slid into the bottom side of the cup where it locks in the center. With the connector pin, the three-component measuring head is attached to a commercial measuring shaft (shaft for disposable measuring systems, D-CP/PP7, No. 10636, Anton Paar) of the rheometer. In between the PTFE ring and cup, an agar layer is inserted. This agar layer is produced in a hat-like geometry using a special PTFE mold (Figure 1b). Because of the
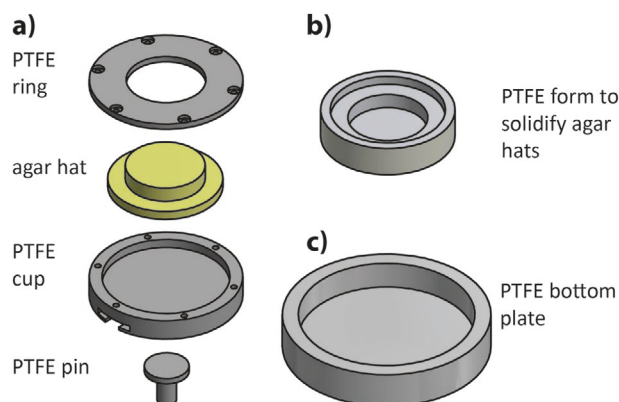

Figure 1. Schematic representation of the custom-made components required for the detachment tests conducted on a commercial rheometer. a) Individual parts of the dedicated measuring head; the ring, cup and pin are made of PTFE, and a hat-shaped agar layer can be inserted in between the cup and the ring. The ring is attached to the cup with screws, and the pin can be slid into the cup and allows for connecting the fully assembled measuring head to the shaft of the rheometer. b) PTFE form used for the preparation of the hat-shaped agar layers. c) PTFE bottom plate that can be filled with an agar layer so that a biofilm can be cultivated on its surface.

hat-like shape, the upper part of this agar piece (having a diameter of 25 mm) protrudes the ring structure of the sample holder; this ensures that only the surface, where the biofilm is cultivated on, is in contact with the bottom plate of the rheometer measuring setup during a measurement. As a bottom plate holding a biofilm sample, a PTFE bowl was designed (Figure 1c); also here, the cavity can be filled with agar onto which biofilm cultivation is easily possible. The cavity in this PTFE bowl has a diameter of 55.2 mm and a height of 9 mm, and the bowl is clamped into the rheometer bottom plate (P-PTD200/80/I, No. 81664467, Anton Paar) for the detachment measurements. CAD models and the images of the custom-made components for the detachment tests were created with Autodesk Inventor Professional 2020 (Autodesk Corp., San Rafael, USA).

2.2. Bacterial Strains and Growth Conditions

Three different *B. subtilis* strains were used in this study: *B. subtilis* 3610[49] was obtained from the lab of Roberto Kolter (Harvard Medical School, USA); *B. subtilis* B-1[50] was obtained from Masaaki Morikawa (Hokkaido University, Japan); *B. subtilis natto* (27E3)[51] was obtained from the Bacillus Genetic Stock Center (BGSC, USA). *B. subtilis* 3610 is found in soil and common used as model bacteria for the properties of bacterial biofilms.[49] *B. subtilis* B-1 is also found in soil, it was isolated from an oil field.[50] *B. subtilis natto* is known from the traditional Japanese dish nattō where it leads to the fermentation of soybeans.[51] All of the investigated bacterial strains are able to form biofilms on solid surfaces. A liquid culture of each bacterial strain was generated by cultivating small pieces of a frozen glycerol stock in 10 mL of 2.5% (w/v) LB medium (Luria/ Miller; Carl Roth GmbH, Karlsruhe, Germany) at 37 °C and at agitation (300 rpm) for ≈18 h. Before the planktonic bacteria were plated onto agar, their OD_{600} was measured with a spectrophotometer (GeneQuantpro, No. 1715,

**ADVANCED
SCIENCE NEWS**

www.advancedsciencenews.com

**ADVANCED
MATERIALS
INTERFACES**

www.advmatinterfaces.de

Amersham Biosciences, Little Chalfont, United Kingdom) and set to 0.5 by diluting the bacterial liquid culture with fresh LB medium. Then, the bacterial suspension was inoculated on 1.5% (w/v) agar-agar (Carl Roth GmbH) by distributing 1.6 µL cm^{-2} of the diluted liquid culture homogeneously over the agar plates. In detail, 100 µL of the liquid culture were added to a commercial petri dish, 40 µL to the custom-made PTFE bowls and 8 µL to the agar hats.

Commercial petri dishes with a diameter of 8.8 cm were used to cultivate biofilm for rheological measurements (for those measurements, larger biofilm amounts were required). Custom made PTFE bowls with a diameter of 5.5 cm were used to cultivate biofilm to determine the biofilm wetting properties and were also used as bottom part of the detachment measurements. For the top part of the detachment tests, agar hats with a diameter of 2.5 cm were used. The thickness of the agar layers in commercial petri dishes, custom-made PTFE bowls and agar hats was always set to ≈8 mm by filling the respective reservoirs with 50, 19, and 6 mL of agar medium, respectively. This ensured that the thickness of biofilm cultivated on those three substrate variants was comparable. The inoculated agar samples were all incubated for 24 h at 37 °C and at high humidity (>80%).

For the tests described in the results section, biofilms were cultivated on different agar media, which differed in the content of nutrients; as "standard" growth conditions, agar enriched with 2.5% (w/v) LB medium (Carl Roth GmbH) was used. For some experiments, the agar substrate was enriched with 0.5 mmol of a selected metal salt by adding sterile-filtered metal salt solutions to autoclaved LB agar at a temperature of 60 °C. The salts used in this study were $CaCl_2$, $CuCl_2$, $ZnCl_2$, $AlCl_3$ (Carl Roth GmbH), and $FeCl_3$ (Sigma Aldrich Corp., Missouri, USA). To examine the influence of metal ion exposure to mature biofilms, biofilms were cultivated at standard conditions as described above. Then, the mature biofilm layer was treated with a solution of $CuCl_2$ (250 mmol) as follows: for the bottom plates, the $CuCl_2$ solution was poured onto the biofilm layer such, that the whole biofilm surface was covered with liquid. Biofilm cultivated on the agar hats were stored upside down (with the biofilm layer facing downward) and immersed into the $CuCl_2$ solution. In either case, the incubation time was 1 h; then the $CuCl_2$ solution was discarded, and the biofilm layer was allowed to dry at room temperature for 10 min so that liquid remnants on the surface could evaporate. In preliminary experiments, it was shown that the different treatment procedure of the petri dishes and agar hats have the same effect on the biofilm properties (Figure S6, Supporting Information). For simulating limiting nutrient conditions, biofilm was cultivated on MSgg agar (0.5% glycerol, 0.5% K-glutamate, 5 mmol K-phosphate, 100 mmol MOPS, 2 mmol $MgCl_2$, 0.7 mmol $CaCl_2$, 0.05 mmol $MnCl_2$, 0.05 mmol $FeCl_3$, 0.001 mmol $ZnCl_2$, 0.002 mmol thiamine, 50 µg mL^{-1} L-tryptophan, 50 µg mL^{-1} L-phenylalanine, 50 µg mL^{-1} threonine), which was prepared at pH 7.0 according to Branda et al.[49]

2.3. Biofilm Wetting Tests

To determine the wetting behavior of the different biofilm samples, a 10 µL droplet of ddH_2O was placed onto the biofilm surface. Then, a transversal image of the liquid–solid interface was captured right afterward using a high-resolution camera (Point Gray Research, Richmond, Canada). The static contact angle value was determined from such pictures, using the software ImageJ and the "drop snake" plug-in.[52] Afterward, superhydrophobic biofilm samples (i.e., those with static contact angles >120°) were tilted and the response of the liquid droplet was observed to distinguish between rose petal (high adhesion: droplet sticks) and lotus-like (low adhesion: droplet rolls off) hydrophobicity. In addition, contact angle hysteresis measurements were conducted as described and summarized in the Supporting Information.

2.4. Rheological Measurements

To determine the rheological properties of the different biofilms, the biofilms were cultivated as described above and harvested from the agar substrate by manual scraping. Rheological measurements were performed using a commercial shear rheometer (MCR 302; Anton Paar) equipped with a 25 mm aluminum measuring head (PP25) and a plate–plate geometry. The plate separation was set to 0.3 mm. A solvent trap was applied to prevent sample drying during the measurements that were realized at 21 °C and in strain-controlled mode. To ensure linear material response, small strains corresponding to a torque of ≈0.5 µN m (this correlates to a shear stress of ≈0.1 Pa) were applied. In every rheological experiment, both the storage and loss modulus were determined over a frequency range of 0.1–10 Hz. Since, in all cases described in this study, the moduli obtained for a given biofilm sample were only weakly dependent on frequency (exemplary frequency spectra for different biofilm samples are shown in the Supporting Information; Figure S7, Supporting Information), only the moduli obtained at a frequency of 1 Hz were considered for obtaining the bar plots in the manuscript. For each condition, at least six samples were tested, which were obtained from two biological replica. For those shear measurements, standard deviations were chosen as error bars, since biological variations between different replicates of the bacterial biofilms always dominate the technical uncertainties/inaccuracies of the measurements. In fact, the technical error, which can be obtained from repeated rheological measurements of the same sample (e.g., a 1.5% (w/v) agar hydrogel), amounts to only <5%: five frequency sweeps conducted with the same agar sample in a range from 0.1 to 10 Hz return a storage modulus of 5058 Pa ± 199 Pa (determined at an intermediate frequency of 1 Hz).

2.5. Detachment Tests

In the presented study, the two material pairings biofilm/aluminum and biofilm/biofilm were investigated. As reference measurements, the material pairings agar/aluminum and agar/agar were used. For both measuring heads, the contact area had a diameter of 25 mm. In each detachment test, first the measuring head was moved down onto the bottom plate at a speed of 100 µm s^{-1} until a normal force of 1 N was reached. This force level was chosen since pretests had shown, that such a normal
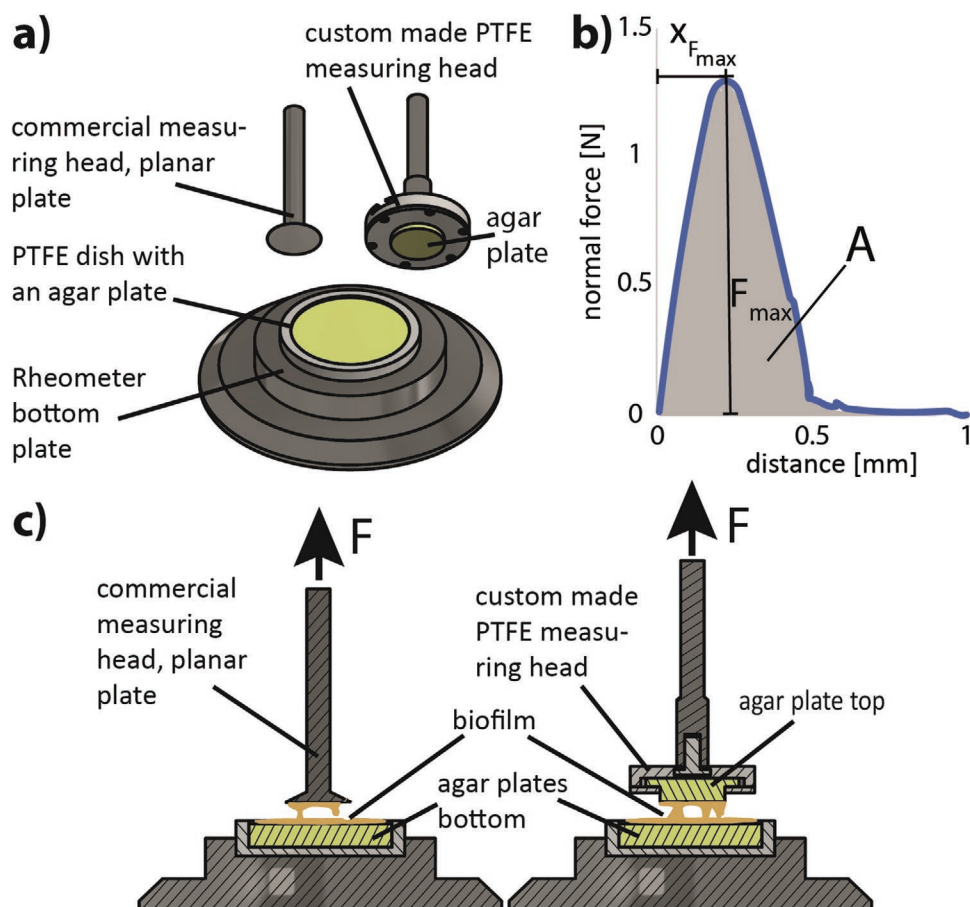
Figure 2. Overview of the two configurations used in the detachment tests. a) The custom-made bottom plate is paired with either a commercial measuring head or the custom-made measuring head described in the main text. b) Typical examples of a force–distance curve obtained during a detachment test. Relevant parameters obtained from such a curve are the maximal force (F_{max}), the distance at which this maximal force occurs (x_{Fmax}) and the area A below the force–distance curve, which corresponds to the separation work. c) Experimental setup for the two material pairings used in this study, i.e., biofilm/aluminum (left) and biofilm/biofilm (right).

force level is sufficient to obtain full contact between the two surfaces without damaging the agar substrate. When this normal force was reached, the position was maintained for 60 s; this allowed the normal force to relax and reach a plateau value. Afterward, the measuring head was lifted up again at a speed of 100 µm s^{-1}, and the force occurring during this pulling process was recorded at a measuring point density of 10 s^{-1} until the measured force dropped to zero (**Figure 2**b). The rheometer used here has a normal force resolution of 0.5 mN, which is valid in a normal force range between 5 mN and 50 N. The measured peak force values of the investigated biofilms range between 50 mN and 3 N, which is at least tenfold larger than the normal force resolution of the device. In addition to these force measurements, the biofilm areas exposed to this normal force treatment were also analyzed optically by imaging them with a digital camera (Samsung Galaxy S7, Samsung Group, Seoul, South Korea). Moreover, after each detachment test, the biofilm layers from the tested surface areas were removed by scraping with a polydimethylsiloxane spatula and weighed with a microbalance (XSE205 Dual Range, d = 0.01 mg/0.1 mg, Mettler Toledo, Columbus, USA). Those amounts were then compared to those collected from untested samples created at the same conditions

by calculating the ratio of treated/untreated samples (using average values of six samples generated from two biological replicates). The material transfer values reported in the results section denote percentage values differences, i.e., a material transfer of 15% corresponds to a loss (or gain) of 15% of biofilm mass on one of the surfaces tested in the respective material pairing.

2.6. Data Evaluation

All error bars shown in the figures denote the standard deviation as calculated from the mean values. In this study, standard deviations were chosen as error bars since, for measurements conducted on naturally grown, biological materials such as bacterial biofilms, the biological variations occurring between different samples always dominate the technical uncertainties/inaccuracies—especially when the tested biofilms were cultivated on different days (which is typically done to explore this biological variability arising from sample generation). For the calculation of all mean values and the corresponding standard deviations, Microsoft Excel 2016 (Microsoft Corporation, Redmond, USA) was used.

3. Results and Discussion

To conduct adhesion/cohesion experiment with bacterial biofilms, a customized sample chamber (see Figure 2a) was developed as described in detail in the Methods section. With this customized setup, it is possible to perform measurements with biofilms grown on either (or both), the lower and upper part of the two-component measuring setup. In the following, if detachment tests are conducted between biofilm and aluminum, biofilm is cultivated only on the bottom part of the measuring setup (Figure 2c, left). In contrast, if detachment tests with two biofilm surfaces are performed, also the upper part of the sample holder contains a biofilm-grown agar layer (Figure 2c, right).

3.1. Measurement Procedure and Possible Modes of Rupture

To assess the reproducibility of the customized setup, we first conduct reference measurements, where the bottom part of the sample holder contains agar only. Detachment tests performed on this agar layer using an aluminum surface as a countermaterial on the measuring head returns maximal adhesion forces, which are well within the range of normal forces the rheometer can accurately determine. In detail, we find $F_{max,alu/agar} = (0.53 \pm 0.15)$ N (Figure S8a, Supporting Information) at a separation distance of (0.14 ± 0.03) mm (Figure S8b, Supporting Information). When an agar surface is used as a countermaterial on the upper part of the measuring setup, the corresponding values are only slightly higher: now, we measure $F_{max,agar/agar} = (0.61 \pm 0.12)$ N (Figure S8c, Supporting Information) at an average separation distance of (0.37 ± 0.11) mm (Figure S8d, Supporting Information). The small fluctuations in the maximal forces determined in those reference measurements can be due to two technical challenges: first, variations in the moisture content of the agar plates can be responsible; second, an imperfect alignment of the bottom part of the sample holder and the upper part (the measuring head) may contribute as well. However, as the sample-to-sample variations in those reference measurements are all rather small, we conclude that the in-house crafted sample holders are functional and that the measuring method is suitable for conducting more complex measurements involving biofilms.

When slimy substances such as biofilms are examined with the method presented here, it is important to distinguish between the different types of fractures that can occur at a biofilm/agar, biofilm/aluminum or biofilm/biofilm interface (Table S1, Supporting Information). One possible scenario is that the measuring head detaches from the biofilm layer (grown on the bottom plate) without damaging the biofilm. In this case, the biofilm will be stretched but remains attached on the agar substrate. The resulting normal force corresponds to the adhesion properties between the biofilm surface and the surface of the measuring head (i.e., either aluminum or biofilm). A second possibility is that the biofilm layer is completely removed from the agar layer it was grown on (i.e., from either the bottom plate or the measuring head); now, transfer of biological material to the other surface should occur at rate of close to 100%. In this case, the reported normal forces describe the adhesion strength of the biofilm to the substrate on which it was cultivated (here: agar). The third option is that the biofilm layer is partially torn apart; then, after a separation experiment, biofilm material should be present on both surfaces, i.e., on the measuring head as well as on the bottom plate. In this scenario, where the biofilm itself is ruptured, the measured normal forces will depend on the internal cohesion strength of the biofilm layer.

With those considerations in mind, we will not only record and compare the peak forces occurring during the different rupture processes, we will also determine the amount of biofilm material transferred to the second surface involved in the detachment test. Together, this approach should allow us to differentiate the three possible fracture types outlined above.

3.2. Viscoelastic Properties and Wetting Behavior of the Studied Biofilms

Before we conduct the first set of detachment experiments with different *B. subtilis* biofilms, we determine the viscoelastic properties and wetting behavior of the three biofilm variants we plan to compare. Our rationale for doing this is that both of those material properties are likely to affect the adhesion behavior of the biofilms. As shown in **Figure 3**, the biofilms we grow from *B. subtilis* 3610 and *B. subtilis* natto are very similar to each other in terms of both, viscoelasticity and wetting (Figure 3a): we measure storage moduli around 1 kPa and hydrophilic surfaces with contact angles between 25° and 40°. In contrast, biofilms grown from *B. subtilis* B-1 bacteria are much softer (here, $G' \approx 100$ Pa) and have strongly hydrophobic surfaces with contact angles as high as 125° (Figure 3a). In detail, these *B. subtilis* B-1 biofilm exhibit rose petal-like hydrophobicity: a wetting water droplet sticks to the surface and does not roll off when the biofilm sample is tilted or turned upside down. In addition to this qualitative method to determine the type of superhydrophobicity, contact angle hysteresis measurements were conducted on all hydrophobic biofilms (Figure S9, Supporting Information). Here, the difference between the contact angles determined at the first and last step of those dynamic wetting tests (ΔCA) was calculated (Table S2, Supporting Information). Furthermore, the topographical structure of the biofilms, which is crucial for the detailed mode of wetting was investigated with laser scanning profilometry (Figure S10, Supporting Information) for each biofilm variant, and the respective metrological roughness parameters (Sq and Sdr values) were calculated (Table S3, see the Supporting Information for details). In full agreement with previous results, we found large differences between hydrophilic biofilms (which exhibit a very smooth and unstructured surface) and the hydrophobic biofilms (which show multiscale roughness on the micro- and nanolevel in addition to mesoscopic waviness).[53] For the detailed wetting behavior of the biofilms (i.e., the type of hydrophobicity: lotus- or rose-like), the roughness features on the micro- and nanoscale are very important; in contrast, the mesoscopic waviness is less relevant, although it contributes to the calculated metrological parameters (for more detailed information, see the Supporting Information).
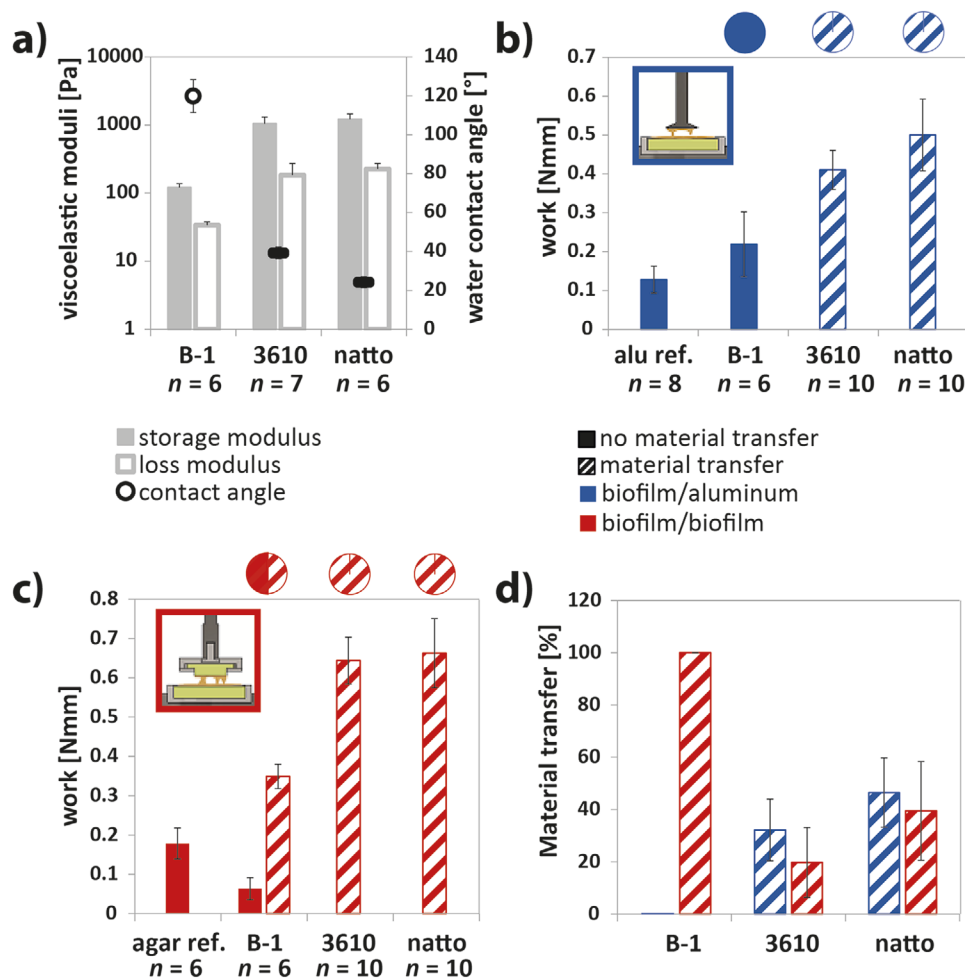
**ADVANCED
SCIENCE NEWS**
www.advancedsciencenews.com

**ADVANCED
MATERIALS
INTERFACES**
www.advmatinterfaces.de

Figure 3. Material properties and detachment behavior of *B. subtilis* B-1, *B. subtilis* 3610 and *B. subtilis* natto biofilms. Data obtained for "empty" material pairings (where no biofilms were grown on the agar layers) are depicted as references. a) Viscoelastic properties and wetting behavior of the biofilms. Full bars denote the storage modulus and open bars the loss modulus. The contact angle is depicted with open circles when rose petal-like hydrophobic behavior is observed, and with filled symbols for hydrophilic behavior. The separation work measured is depicted for the material pairing biofilm/aluminum b) and for the material pairing biofilm/biofilm c). Full bars denote absence of material transfer whereas striped bars indicate that material transfer did occur. The pie charts above the bars visualize how often material transfer occurred for a given sample type. The amount of biofilm material transferred during a detachment test is summarized in (d). All data shown represent mean values; error bars denote the standard deviation. The number of different samples analyzed per condition is specified in the respective subfigures.

Interestingly, we also find differences between the three biofilm variants when we compare results from the detachment measurements. For both types of material pairing, i.e., for biofilm/aluminum (Figure 3b) and biofilm/biofilm (Figure 3c) configurations, the measurements conducted with *B. subtilis* 3610 and *B. subtilis* natto biofilms return higher values for the work needed to achieve full separation of the two surfaces than for *B. subtilis* B-1 biofilm. In detail, the maximal force occurring during the detachment test as well as the distance, at which this force peak is located, is higher for *B. subtilis* 3610 and *B. subtilis* natto biofilms than for *B. subtilis* B-1 biofilm (Figure S8, Supporting Information).

When we examine the material transport occurring as a consequence of the detachment process (Figure 3d), again *B. subtilis* B-1 biofilms stand out. For the material pairing biofilm/aluminum, *B. subtilis* 3610 and *B. subtilis* natto biofilms show such material transport (and at comparable levels), but B-1

biofilms do not. This indicates that the first two biofilm variants exhibit cohesive failure when probed with an aluminum surface, whereas, in the case of B-1 biofilms, adhesive failure dominates. For the material pairing biofilm/biofilm, we find similar levels of material transfer for *B. subtilis* 3610 and *B. subtilis* natto biofilms as for the biofilm/aluminum pairing. This indicates that, also here, a cohesion failure occurs. However, also in this biofilm/biofilm configuration, *B. subtilis* B-1 biofilms return a different result: Here, two different scenarios are observed: Either the two B-1 biofilm surfaces are separated from each other without any material transfer or there is a complete material transfer from one side to the other. In either case, this indicates an adhesion failure, which takes place between the two biofilm layers (=no material transfer) or between the biofilm layer and the agar substrate (=full material transfer).

These first results allow us to conclude that the viscoelastic properties as well as the wetting behavior of biofilms seem to

be relevant for rationalizing the observed differences in the detachment tests conducted with *B. subtilis* 3610 and *B. subtilis natto* biofilms on the one hand and *B. subtilis* B-1 biofilms on the other hand. It seems that hydrophilic biofilms exhibit stronger adhesion to foreign surfaces than hydrophobic biofilms, and that they are more likely to stick to each other. However, the higher shear stiffness of *B. subtilis* 3610 and *B. subtilis natto* biofilms could also result in stronger cohesion of these biofilms, which can influence the detachment tests as well.

To disentangle the influence of these two biofilm properties on the adhesion and detachment process, we conduct further experiments where we attempt to alter only one of those properties for a given biofilm variant without modifying the other one. To achieve this, we repeat detachment tests with *B. subtilis* B-1 biofilm, but generate the biofilm such that its viscoelastic properties are modified. *B. subtilis* B-1 biofilms are chosen for this purpose since previous studies[34,37] have already shown that the stiffness of those biofilms can be drastically changed by metal cations. This can be achieved by either treating mature biofilms with aqueous solutions containing such metal cations (which leads to a formation of chelate complexes between the cations and the biomacromolecules from the biofilm matrix thus inducing biofilm stiffening) or by enriching the growth medium used for biofilm generation with metal ions; the latter approach affects the stiffness and/or wettability of biofilms by influencing the production of biofilm matrix components. Another method to alter the stiffness and/or wettability of a biofilm is to cultivate the biofilm with different growth media, e.g., on MSgg agar.[54,55] In the following, we explore those three options to obtain biofilms with altered wetting behavior and/or viscoelastic properties.

3.3. Exposure to Metal Cations during Biofilm Growth

We first study *B. subtilis* B-1 biofilms cultivated on LB agar in the presence of metal cations. To ensure that the added ions have no toxic effect on the bacteria so that they are still able to form a proper biofilm, the ion concentrations are kept at low levels, i.e., at 0.5 mmol. As expected, the addition of those metal ions has an influence on both, the viscoelastic properties and the wetting behavior of the biofilms (**Figure 4**a). The addition of Cu^{2+} and Zn^{2+} slightly increases the storage modulus of the biofilm, whereas the addition of Fe^{3+} slightly reduces the biofilm stiffness. The other two tested ions, Al^{3+} and Ca^{2+} do not influence the viscoelastic properties of B-1 biofilms. Regarding the wetting behavior of the biofilms, we find that—overall—the strongly hydrophobic surface properties of the biofilm are maintained. Yet, the contact angles we measure on biofilms cultivated on metal ion-enriched agar substrates are all slightly higher than those we determine when standard agar substrates are used. In addition, for biofilm grown on Cu^{2+} or Al^{3+} enriched agar, the mode of superhydrophobicity is affected; here, a lotus-like behavior is developed—at least on some parts of the biofilm surface. In other words, now, there are areas on the biofilm surface where a water drop easily rolls off when the biofilm sample is tilted.

In addition to those differences in the viscoelastic and wetting properties, we also find differences in the adhesion

behavior of those biofilms grown in the presence of metal ions. For the material pairing biofilm/aluminum, we observe a reduction in the separation work for all those modified biofilms (Figure 4b). Interestingly, we find the strongest reduction of the separation work for biofilms grown in the presence of Cu^{2+} and Zn^{2+}—and among the cations we test here, those two increase the stiffness of B-1 biofilms. Moreover, no material transfer occurs in any of these new tests conducted with modified B-1 biofilms. This suggests that, now, adhesion failure is the dominant mechanism during the detachment process.

We interpret this finding such that—with an increased biofilm stiffness—two parameters relevant for the mechanical failure process are affected: first, the material can endure larger forces until it ruptures; second, the biofilm material can transfer the externally applied stretching/pulling forces to its substrate more efficiently thus rendering an adhesion failure more likely. Of course, also the alteration of the biofilm surface properties we observe could, in principle, contribute to the observed differences in the detachment tests. However, as the countersurface used in this set of experiments is hydrophilic aluminum, the subtle change in the mode of biofilm superhydrophobicity we find here appears to be a rather unlikely candidate for rationalizing the absence of material transfer we describe above.

When we test the same set of metal-ion exposed biofilms in the biofilm/biofilm configuration, the mode of fracture changes. Untreated biofilms show either complete material transfer or no material transfer at all—and both outcomes are similarly likely. In both cases, an adhesion failure takes place; in the first scenario, it occurs on the substrate, whereas, in the second scenario, it occurs between the two biofilm surfaces. For biofilms exposed to metal ions, material transfer events occur less frequently (Figure 4c). Only biofilms exposed to Al^{3+} or Zn^{2+} exhibit partial material transfer events (Figure 4d), and only in ≈1/3 of the conducted tests. As we argued above, such a partial material indicates a mixed detachment event combining adhesion and cohesion failure. This finding is in agreement with our observation that ionic cross-linking of the biofilm matrix as brought about by the metal cations slightly increases the biofilm stiffness. In addition, such cross-linking effects are also likely to increase the cohesive strength of the biofilm matrix thus rendering a cohesion failure less likely.

Consistent with this picture, we also find a reduction of the separation work for almost all biofilm variants exposed to metal ions. We observe the strongest effect for biofilms cultivated on LB agar enriched with Cu^{2+} and Al^{3+}—and these are the biofilms, where we also find an alteration in their mode of surface hydrophobicity.

3.4. Treatment of Mature Biofilms with Metal Cations

When a mature biofilm of *B. subtilis* B-1 is exposed to Cu^{2+} ions, the properties of the biofilm are changed a lot. However, different from the experiments described above, where the biofilm was exposed to cations during growth—the cations now do not change the composition of the biofilm. Instead, the metal ions lead to the formation of chelate complexes and thus introduce ionic crosslinks between the biofilm biomacromolecules.[37]
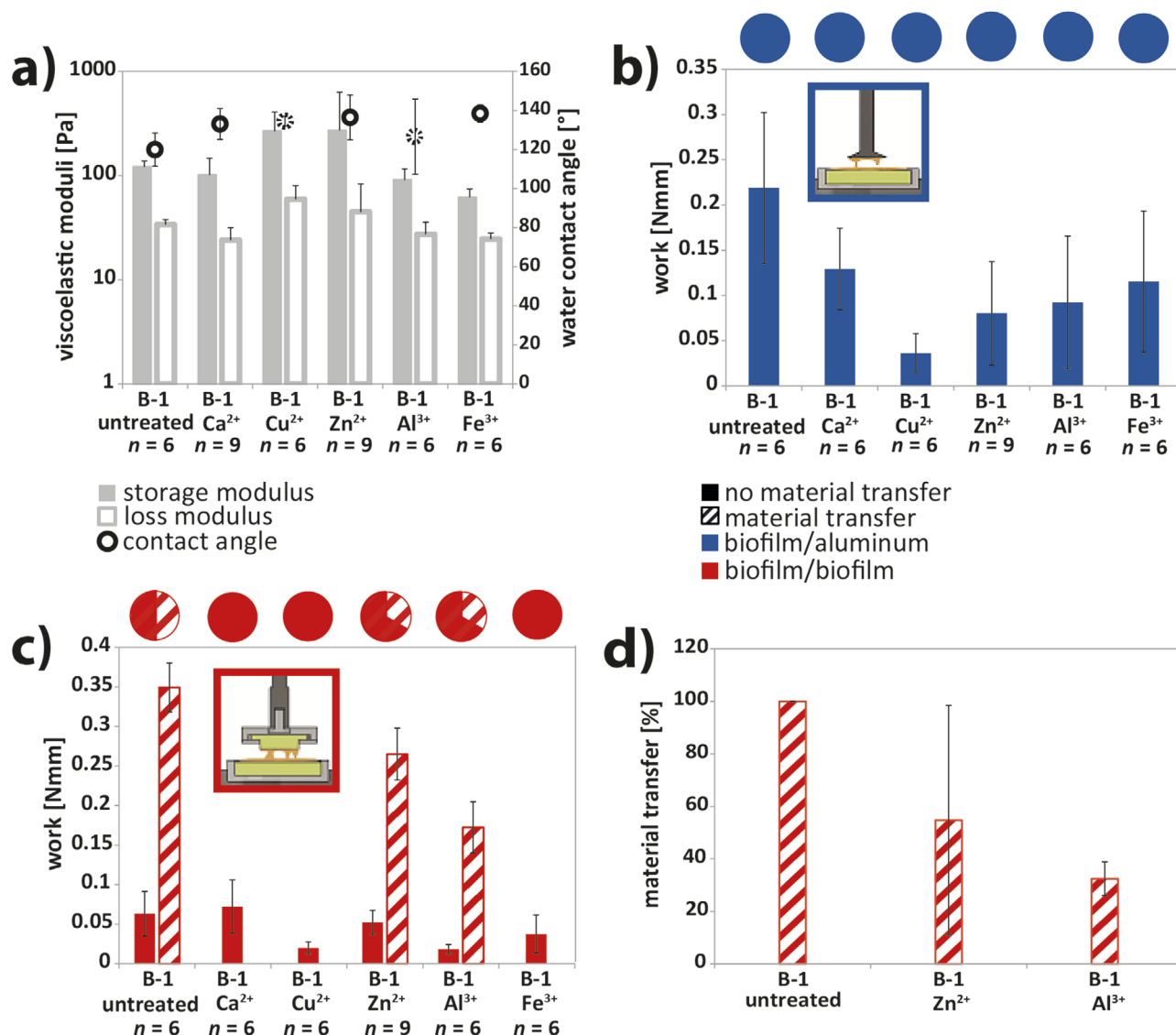
Figure 4. Material properties and detachment behavior of *B. subtilis* B-1 biofilms treated with metal ions during growth; data obtained for samples grown at standard conditions is shown as a reference. a) Viscoelastic properties and wetting behavior of the biofilms. Full bars denote the storage modulus and open bars the loss modulus. The contact angle is depicted with open circles when rose petal-like hydrophobic behavior is observed, and with dashed circles when partial rose-like and partial lotus-like hydrophobic behavior occurred. The separation work measured is depicted for the material pairing biofilm/aluminum b) and for the material pairing biofilm/biofilm c). Full bars denote absence of material transfer whereas striped bars indicate that material transfer did occur. The pie charts above the bars visualize how often material transfer occurred for a given sample type. The amount of biofilm material transferred during a detachment test is summarized in (d). All data shown represent mean values; error bars denote the standard deviation. The number of different samples analyzed per condition is specified in the respective subfigures.

As demonstrated before,[34,37] such a formation of chelate complexes strongly increases the stiffness of the biofilm. And indeed, the same effect is observed here (**Figure 5**a): after exposure to Cu^{2+} ions, the storage modulus of the biofilm sample is increased by three orders of magnitude to ≈100 kPa. Yet, with this particular treatment, the wetting behavior of the biofilm remains unchanged.

For the material pairing biofilm/aluminum, most samples show the expected behavior, i.e., detachment without material transfer and a slightly higher separation work than for untreated B-1 biofilms. In line with our argumentation above, both features can be explained by the increased stiffness of the

biofilm material. Interestingly, some of those Cu^{2+}-exposed B-1 biofilms show a qualitatively altered detachment behavior: in ≈1/3 of the experiments, partial material transfer occurs; in contrast, untreated B-1 biofilm do not show any material transfer events (Figure 5b,d). In other words, now cohesive failure contributes as well. This change in the mode of fracture was unexpected since stiff biofilms—so far—showed mostly adhesive failure, and hydrophobic biofilms appeared to have a low stickiness toward aluminum. Yet, it is important to realize that, as a consequence of the treatment procedure applied here (where a $CuCl_2$ solution is poured onto the biofilm surface and then removed again after a certain incubation time), the biofilm
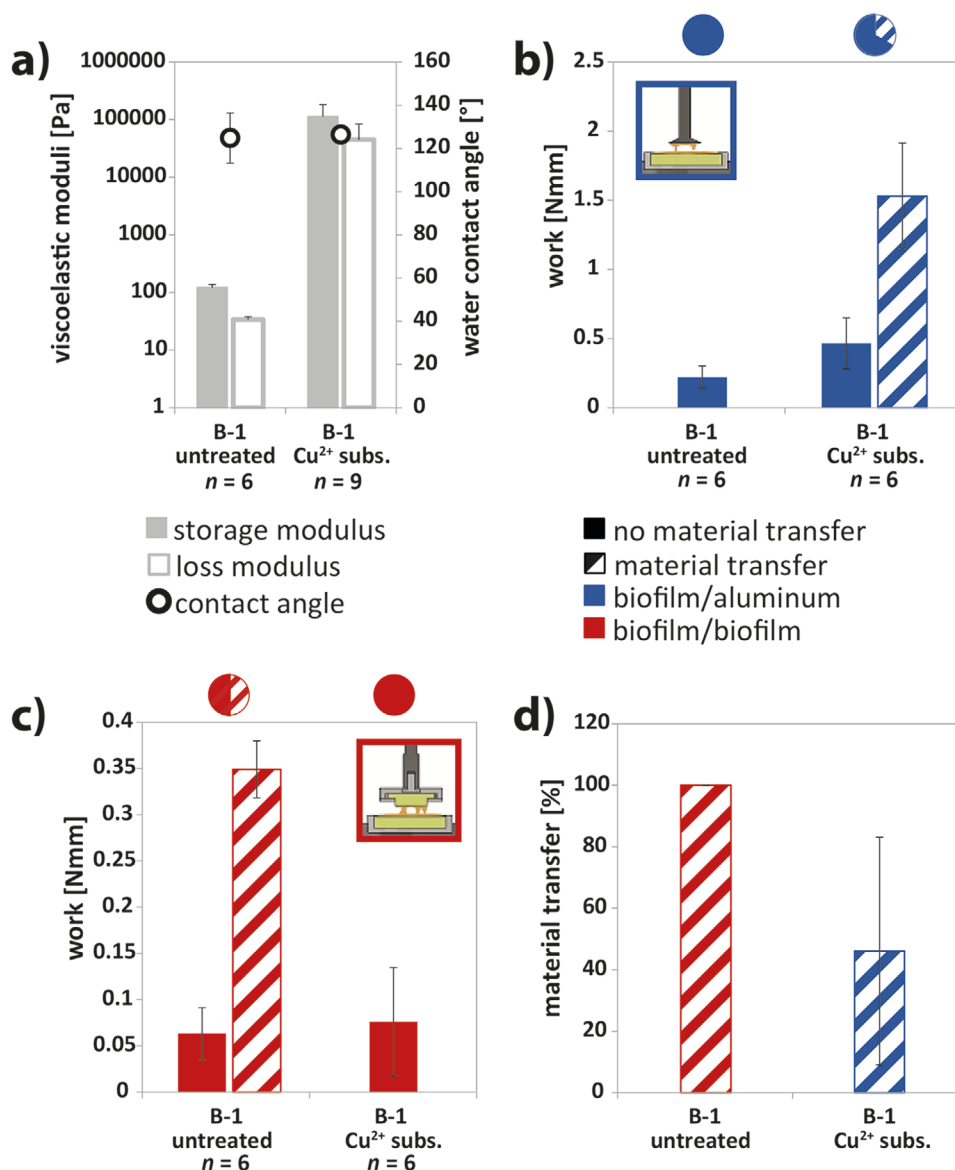
Figure 5. Material properties and detachment behavior of mature *B. subtilis* B-1 biofilms treated with a CuCl₂ solution; data obtained for samples grown at standard conditions is shown as a reference. a) Viscoelastic properties and wetting behavior of the biofilms. Full bars denote the storage modulus and open bars the loss modulus. The contact angle is depicted with open circles for rose petal-like hydrophobic behavior. The separation work measured is depicted for the material pairing biofilm/aluminum b) and for the material pairing biofilm/biofilm c). Full bars denote absence of material transfer whereas striped bars indicate that material transfer did occur. The pie charts above the bars visualize how often material transfer occurred for a given sample type. The amount of biofilm material transferred during a detachment test is summarized in (d). All data shown represent mean values; error bars denote the standard deviation. The number of different samples analyzed per condition is specified in the respective subfigures.

surface is wetted. Remaining moisture on those biofilm samples could be responsible for those unexpected adhesion effects with the aluminum surface. Moreover, we also observe that the aluminum surface of the measuring head used for the rheology and detachment tests shows signs of corrosion (Figure S11, Supporting Information)—and we attribute this to direct contact of residual Cu^{2+} ions from the biofilm surface with the aluminum material: such residual Cu^{2+} ions on the biofilm surface may act as ionic cross-linkers with the aluminum surface thus giving rise to higher adhesion forces inducing material transfer. Alternatively, the partially corroded aluminum surface

exhibits a higher surface roughness promoting adhesion to the biofilm (Figure S11, Supporting Information). Consistent with any of those two possibilities, the measured separation work is strongly increased as a consequence of the Cu^{2+} exposure.

For the material pairing biofilm/biofilm (Figure 5c), a different picture emerges. Whereas untreated biofilms show material transfer in 50% of the measurements, this feature does not occur anymore when the *B. subtilis* B-1 biofilm is treated with Cu^{2+}. In other words, now adhesion failure dominates, which fully agrees with the line of argumentation we followed so far.
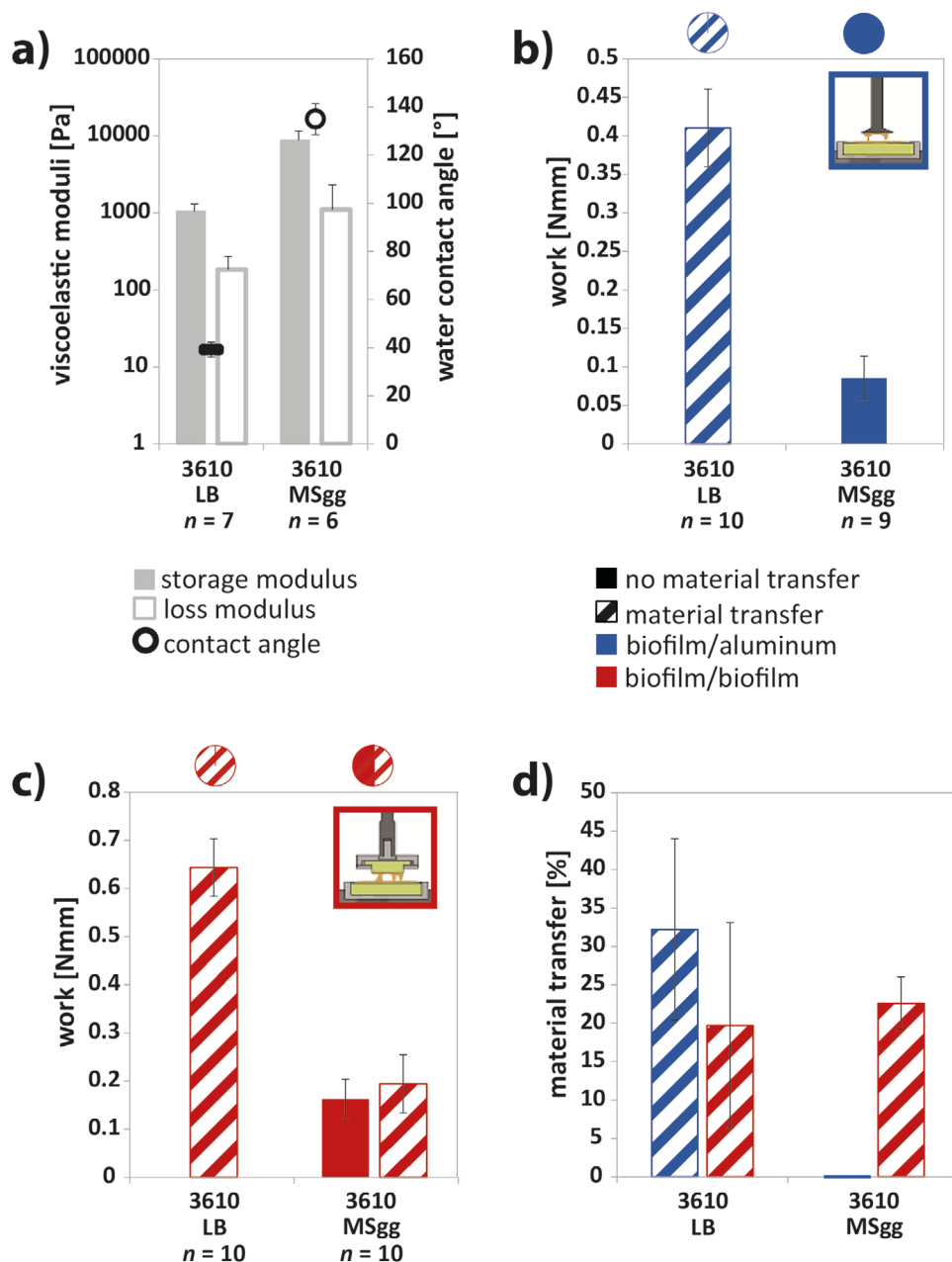
Figure 6. Material properties and detachment behavior of *B. subtilis* 3610 biofilms cultivated on MSgg agar, where nutrients are limited; data obtained for samples grown at standard conditions (=on LB agar) is shown as a reference. a) Viscoelastic properties and wetting behavior of the biofilms. Full bars denote the storage modulus and open bars the loss modulus. The contact angle is depicted with open circles when rose petal-like hydrophobic behavior is observed, and with filled symbols for hydrophilic behavior. The separation work measured is depicted for the material pairing biofilm/aluminum b) and for the material pairing biofilm/biofilm c). Full bars denote the absence of material transfer whereas striped bars indicate that material transfer did occur. The pie charts above the bars visualize how often material transfer occurred for a given sample type. The amount of biofilm material transferred during a detachment test is summarized in (d). All data shown represent mean values; error bars denote the standard deviation. The number of different samples analyzed per condition is specified in the respective subfigures.

3.5. Biofilm Cultivation during Nutrient Limitation

The last option we explore to alter the physical properties of the biofilm is limiting the nutrient availability during biofilm growth. Different from B-1 biofilms (whose wetting behavior cannot be altered easily by this approach), *B. subtilis* 3610 biofilms exhibit wetting properties that sensitively depend on the nutrient source.[54] This behavior is reproduced here: when grown on MSgg agar, those biofilms possess rose petal-like hydrophobicity (**Figure 6**a); at the same time, the stiffness of the biofilm is increased by one order of magnitude compared to cultivation on LB agar.

As consequence of these changes in the biofilm properties, we expect the biofilm to be less adhesive toward foreign
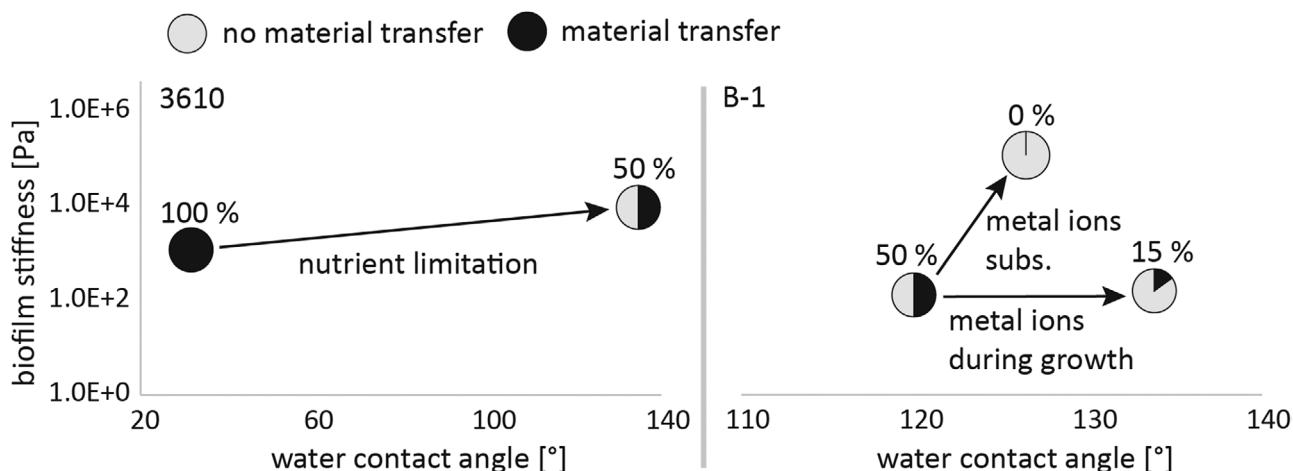
Figure 7. Relation between the material properties of the tested biofilms and the occurrence of material transfer during detachment tests conducted in the biofilm/biofilm configuration for 3610 biofilms (left) and B-1 biofilms (right). Data obtained at comparable conditions (similar biofilms, similar treatments, similar properties) were pooled. Black color denotes samples where material transfer occurred (and their fraction within a set of samples is referred to by the percentage values shown above the pie charts); gray color denotes samples, which did not show such material transfer.

surfaces and to be more difficult to rupture; in other words, we expect that those MSgg grown biofilm samples should tend to show adhesion failure without material transfer in the detachment tests. Indeed, this is what we observe for both, the material pairing biofilm/aluminum (Figure 6b) as well as the biofilm/biofilm configuration (Figure 6c). For the biofilm/aluminum pairing, no material transfer occurs anymore (this was always the case when the same biofilm was cultivated on LB agar) and adhesion failure clearly is the dominant mode of fracture. For the biofilm/biofilm pairing, we observe a similar trend—yet less pronounced: here, a material transfer occurs less often than when LB agar is used for biofilm cultivation, i.e., only in ≈1/2 of the experiments. Consistent with our expectation, we also find a cohesion failure here when no material transfer occurs; if such material transfer takes place, however, we find a mixed failure mode with only partial material transfer (Figure 6d). We interpret this finding such that the strong alteration in wetting behavior is mainly responsible for the observed alteration in biofilm adhesion and failure mode; of course, the increase in biofilm stiffness that accompanies the alteration in wetting may also contribute.

In summary, we could show that the measurement technic developed here is suitable for characterizing adhesive properties of bacterial biofilms toward metal surfaces and other biofilm surfaces alike. Two advantages of the method presented here are that this technique applies a uniform stress to the biofilm surface by controlling the normal force acting on the biofilm sample; this approach is very similar to established test protocols used for measuring the tensile strength of technical adhesives, and allows for characterizing the adhesive properties of biofilms in situ. Moreover, the experiments conducted here demonstrated that the adhesive properties and the fracture behavior of different biofilms generated by *B. subtilis* can be altered by changing the biofilm growth conditions or by exposing mature biofilms to cross-linking metal ions. Overall, we observed that two material properties of biofilms, i.e., the biofilms stiffness and the wetting behavior of the biofilm surface, affect the detailed adhesion behavior and failure

mode: Biofilms with a low stiffness and hydrophilic surfaces tend to exhibit a material transfer and thus mostly cohesion fractures whereas biofilms with a high stiffness and hydrophobic surfaces tend to show no material transfer and thus adhesion fractures (**Figure 7**).

At this point of research, there is no suitable theoretical model available to quantitatively rationalize the results obtained here. This is due to two main reasons: first, the intrinsic complexity of the material response of bacterial biofilms (which tend to show different types of nonlinear effects at large stress levels) is high;[38,40] second, the detailed configuration of our measurement setup would need to be accounted for in such a model, and this is not trivial either. For instance, the stress distribution across the biofilm layer (which is located between the two counterparts of the experimental setup) is dependent on various factors, such as the mechanical load distribution and the stiffness of the involved counterparts. To account for the latter two issues, probably a whole different set of experiments will be necessary – most likely also involving FE-based simulations.

Even though we here focused on biofilms generated by *B. subtilis* in combination with either other biofilm layers or aluminum surfaces exposed to air, the presented method can easily be extended further to study other material pairings or environments. For instance, the custom-made measuring head cannot only be equipped with an agar layer, but can also be adjusted to hold other materials such as ceramics or polymer materials (used in medical engineering), hydroxyapatite (as a model for teeth) or even tissue samples. Similarly, also the bottom sample holder of the rheometer could be modified to such that it holds biofilm samples harvested from their natural environment—provided that the substrate carrying the biofilm layer is sufficiently flat. Moreover, the measuring setup could be complemented with a cylindrical chamber such that the detachment process is conducted in a liquid environment; this would make it possible to test the adhesive properties of biofilms grown under water, e.g., those generated from marine bacteria. Finally, conducting those detachment tests on a

**ADVANCED
SCIENCE NEWS**

www.advancedsciencenews.com

**ADVANCED
MATERIALS
INTERFACES**

www.advmatinterfaces.de

commercial research rheometer makes it also easily possible to control selected environmental conditions, such as changes the ambient temperature or humidity.

4. Conclusion

Very often, biofilms are problematic for humans; for example, when they induce clogging or corrosion of pipes.[10,11] However, biofilms can also perform beneficial tasks, e.g., in wastewater treatment where they remove specific pollutants from the water.[56] Whether combating unwanted biofilms or when trying to employ them for human purposes, it is helpful to assess principles that govern the surface adhesion behavior of biofilms. With such knowledge and suitable, standardizable measurement protocols that quantify this material property, it should be possible to develop strategies that either enhance or reduce the adhesion properties of biofilms and other, slimy biomaterials.

Supporting Information

Supporting Information is available from the Wiley Online Library or from the author.

Conflict of Interest

The authors declare no conflict of interest.

Author Contributions

M.K. and O.L. planned the experiments, which were conducted and analyzed by M.K. and C.A.S. The manuscript was written by M.K. and O.L.

[1] G. O'Toole, H. B. Kaplan, R. Kolter, *Annu. Rev. Microbiol.* **2000**, *54*, 49.

[2] H. Vlamakis, Y. Chai, P. Beauregard, R. Losick, R. Kolter, *Nat. Rev. Microbiol.* **2013**, *11*, 157.

[3] H. C. Flemming, J. Wingender, U. Szewzyk, P. Steinberg, S. A. Rice, S. Kjelleberg, *Nat. Rev. Microbiol.* **2016**, *14*, 563.

[4] A. Marguier, N. Poulin, C. Soraru, L. Vonna, S. Hajjar-Garreau, P. Kunemann, A. Airoudj, G. Mertz, J. Bardon, M. Delmée, V. Roucoules, D. Ruch, L. Ploux, *Adv. Mater. Interfaces* **2020**, *7*, 2000179.

[5] H. Cao, O. Habimana, A. Safari, R. Heffernan, Y. Dai, E. Casey, *npj Biofilms Microbiomes* **2016**, *2*, 1.

[6] S. C. Booth, I. F. S. George, D. Zannoni, M. Cappelletti, G. E. Duggan, H. Ceri, R. J. Turner, *Metallomics* **2013**, *5*, 723.

[7] A. Bridier, R. Briandet, V. Thomas, F. Dubois-Brissonet, *Biofouling* **2011**, *27*, 1017.

[8] S. Aggarwal, R. M. Hozalski, *Langmuir* **2012**, *28*, 2812.

[9] A. W. Cense, E. A. G. Peeters, B. Gottenbos, F. P. T. Baaijens, A. M. Nuijs, M. E. H. van Dongen, *J. Microbiol. Methods* **2006**, *67*, 463.

[10] I. B. Beech, J. Sunner, *Curr. Opin. Biotechnol.* **2004**, *15*, 181.

[11] A. Vigneron, E. B. Alsop, B. Chambers, B. P. Lomans, I. M. Head, N. Tsesmetzis, *Appl. Environ. Microbiol.* **2016**, *82*, 2545.

[12] M. Wilson, *Sci. Prog.* **2001**, *84*, 235.

[13] L. Liu, H. Shi, H. Yu, S. Yan, S. L. Biomater, *Science* **2020**, *8*, 4074.

[14] G. Zhang, X. Zhang, Y. Yang, H. Zhang, J. Shi, X. Yao, X. Zhang, *Adv. Mater. Interfaces* **2020**, *7*, 1901706.

[15] Q. Xie, H. Zeng, Q. Peng, C. Bressy, C. Ma, G. Zhang, *Adv. Mater. Interfaces* **2019**, *6*, 1900535.

[16] R. D. Monds, G. A. O'Toole, *Trends Microbiol.* **2009**, *17*, 73.

[17] E. S. Gloag, G. K. German, P. Stoodley, D. J. Wozniak, *Sci. Rep.* **2018**, *8*, 1.

[18] H.-C. Flemming, J. Wingender, *Nat. Rev. Microbiol.* **2010**, *8*, 623.

[19] S. S. Branda, Å. Vik, L. Friedmann, R. Kolter, *Trends Biotechnol.* **2005**, *13*, 20.

[20] I. W. Sutherland, *Trends Biotechnol.* **2001**, *9*, 222.

[21] P. S. Stewart, J. W. Costerton, *Lancet* **2001**, *358*, 135.

[22] C. B. Whitchurch, T. Tolker-Nielsen, P. C. Ragas, J. S. Mattick, *Science* **2002**, *295*, 1487.

[23] Y. Liu, S. F. Yang, Y. Li, H. Xu, L. Qin, J. H. Tay, *J. Biotechnol.* **2004**, *110*, 251.

[24] H. Fan, Z. Guo, *Biomater. Sci.* **2020**, *8*, 1502.

[25] F. Alam, S. Kumar, K. M. Varadarajan, *ACS Biomater. Sci. Eng.* **2019**, *5*, 2093.

[26] M. A. M. van Loosdrecht, J. Lyklema, W. Norde, A. J. B. Zehnder, *Microb. Ecol.* **1989**, *17*, 1.

[27] R. Helbig, D. Günther, J. Friedrichs, F. Rößler, A. Lasagni, C. Werner, *Biomater. Sci.* **2016**, *4*, 1074.

[28] W. M. Dunne, *Clinical Microbiology Reviews* **2002**, *15*, 155.

[29] T. R. Garret, M. Bhakoo, Z. Zhang, *Prog. Nat. Sci.* **2008**, *18*, 1049.

[30] I. Klapper, J. Dockery, *Phys. Rev. E* **2006**, *74*, 031902.

[31] M. G. Mazza, *J. Phys. D: Appl. Phys.* **2016**, *49*, 203001.

[32] S. Tsuneda, H. Aikwa, H. Hayashi, A. Yuasa, A. Hirata, *FEMS Microbiol. Lett.* **2003**, *223*, 287.

[33] A. Harimawan, Y. P. Tin, *Colloids Surf., B* **2016**, *146*, 459.

[34] S. Grumbein, M. Opitz, O. Lieleg, *Metallomics* **2014**, *6*, 1441.

[35] S. Kesel, S. Grumbein, I. Gümperlein, M. Tallawi, A.-K. Marel, O. Lieleg, M. Opitz, *Appl. Environ. Microbiol.* **2016**, *82*, 2424.

[36] M. Klotz, M. Kretschmer, A. Goetz, S. Ezedam, O. Lieleg, M. Opitz, *RSC Adv.* **2019**, *9*, 11521.

[37] M. Kretschmer, O. Lieleg, *Biomater. Sci.* **2020**, *8*, 1923.

[38] O. Lieleg, M. Caldara, R. Baumgärtel, K. Ribbeck, *Soft Matter* **2011**, *7*, 3307.

[39] A. Di Stefano, E. D'Aurizio, O. Trubiani, R. Grande, E. Di Campli, M. Di Giulio, S. Di Bartolomeo, P. Sozio, A. Iannitelli, A. Nostro, L. Cellini, *Microb. Biotechnol.* **2009**, *2*, 634.

[40] S. Jana, S. G. V. Charlton, L. E. Eland, J. G. Burgess, A. Wipart, T. P. Curtis, J. Chen, *npj Biofilms Microbiomes* **2020**, *6*, 1.

[41] L. Pavlovsky, J. G. Younger, M. J. Solomon, *Soft Matter* **2013**, *9*, 122.

[42] G. Habenicht, *Kleben: Grundlagen, Technologien, Anwendungen*, Springer, Berlin **2006**.

[43] DIN EN Vol. 15870, Klebstoffe—Bestimmung der Zugfestigkeit von Stumpfklebungen (ISO 6922:1987 modifiziert), Deutsche Fassung, p. 2009-08.

[44] DIN EN 1465, Klebstoffe—Bestimmung der Zugscherfestigkeit von Überlappungsklebungen, Deutsche Fassung, p. 2009-07.

[45] ISO 11003-Vol. 2:2019-06, Adhesives—Determination of shear behaviour of structural adhesives: Part 2. Tensile test method using thick adherends.

[46] ISO 10033-1:2011-04, Laminated Veneer Lumber (LVL)—Bonding quality: Part 1. Test methods.

[47] M. J. Chen, Z. Zhang, T. R. Bott, *Biotechnol. Tech.* **1998**, *12*, 875.

[48] J. Yan, A. Moreau, S. Khodaparast, A. Perazzo, J. Feng, C. Fei, S. Mao, S. Mukherjee, A. Košmrlj, N. S. Wingreen, B. L. Bassler, H. A. Stone, *Adv. Mater.* **2018**, *30*, 1804153.

[49] S. S. Branda, J. E. González-Pastor, S. Ben-Yehuda, R. Losick, R. Kolter, *Proc. Natl. Acad. Sci. USA* **2001**, *98*, 11621.

[50] M. Morikawa, M. Ito, T. Imanaka, *J. Ferment. Bioeng.* **1992**, *74*, 255.

[51] A. Goto, M. K. Bioscience, *Biotechnol. Biochem.* **1992**, *56*, 1031.

[52] A. F. Stalder, G. Kulik, D. Sage, L. Barbieri, P. Hoffmann, *Colloids Surf., A* **2006**, *286*, 92.

[53] C. F. Garcia, F. Stangl, A. Götz, W. Zhao, S. A. Sieber, M. Opitz, O. Lieleg, *Biomater. Sci.* **2019**, *7*, 220.

[54] M. Werb, C. F. Garcia, N. C. Bach, S. Grumbein, S. A. Sieber, M. Opitz, O. Lieleg, *npj Biofilms Microbiomes* **2017**, *3*, 1.

[55] C. F. Garcia, M. Kretschmer, C. N. Lozano-Andrade, M. Schönleitner, A. Dragoš, Á. T. Kovács, O. Lieleg, *npj Biofilms Microbiomes* **2020**, *6*, 1.

[56] W. K. Shieh, J. D. Keenan, *Bioproducts*, Springer, Berlin **1986**.